



Since January 2020 Elsevier has created a COVID-19 resource centre with free information in English and Mandarin on the novel coronavirus COVID-19. The COVID-19 resource centre is hosted on Elsevier Connect, the company's public news and information website.

Elsevier hereby grants permission to make all its COVID-19-related research that is available on the COVID-19 resource centre - including this research content - immediately available in PubMed Central and other publicly funded repositories, such as the WHO COVID database with rights for unrestricted research re-use and analyses in any form or by any means with acknowledgement of the original source. These permissions are granted for free by Elsevier for as long as the COVID-19 resource centre remains active.



Research paper

Integrating *in silico* and *in vivo* approach for investigating the role of polyherbal oil in prevention and treatment of COVID-19 infection

Amul S. Bahl^{a,1}, Vipin Kumar Verma^{b,1}, Jagriti Bhatia^b, Dharamvir Singh Arya^{b,*}^a Department of Research, Development and Innovation, God's Own Store LLP, Delhi, India^b Department of Pharmacology, All India Institute of Medical Sciences, New Delhi, 110029, India

ARTICLE INFO

Keywords:

Anti-inflammatory
 COVID-19
 GC-MS
 Molecular docking
 Polyherbal oil
 Therapeutics

ABSTRACT

Currently, there are no FDA approved antiviral drugs available to treat COVID-19 patients. Also, due to emergence of new SARS-CoV-2 variants, the protective efficacy of vaccines could be reduced, hence it is urgent to have alternative treatments for combating the SARS-CoV-2 infection. Since, there is a long-standing history of herbal medicine in the treatment of respiratory diseases. In the present study, we investigated two polyherbal oil blend viz. Sudarshan AV and Elixir AV (SAV and EAV) in inhibiting SARS-COV-2. From GC-MS analysis of polyherbal oils (SAV and EAV) a total of 11 active compounds were selected, on the basis of their abundance and activity. Further, from the molecular docking studies, we found an inhibitory effect of these compounds on viral envelope and membrane, spike proteins whilst an agonistic effect with human host receptor angiotensin-converting enzyme 2 (ACE2) implicating the crucial role of the individual compound in resistance of SARS-CoV-2.

Since, the *in-silico* results suggest that polyherbal oil (SAV and EAV) contributes in preventing the entry of SARS-CoV-2 into the human body, we further investigated the efficacy of polyherbal formulated essential oil (FEO; SAV & EAV) in prevention and treatment of COVID-19 in hamster model. The male golden Syrian hamsters (n = 23) were divided into 5 groups i.e., Group 1: Control (n = 3); Group 2: Infected (n = 5); Group 3: Infected + Remdesivir (n = 5); Group 4: Infected + FEO (n = 5) and Group 5: Prophylactic FEO + Infected (n = 5). In both treatment and prophylactic groups, the FEO's significantly reduced the lung injury investigated histopathologically and viral load expression measured by real time PCR in comparison to infected hamsters. Furthermore, cytokines expression analysis clearly highlighted the efficacy of FEO's due to its anti-inflammatory activity and overall protection in treatment groups. In conclusion, the FEO (SAV & EAV) seem to be potent in both prevention and treatment of COVID-19 and related lung injury.

1. Introduction

In December 2019, an outbreak of novel contagious respiratory illness was first reported in Wuhan, China and later escalated into pandemic worldwide [1,2]. The world health organization named this disease as "COVID-19" and was found to be caused by severe acute respiratory syndrome coronavirus 2 (SARS-CoV-2) belongs to the family Coronaviridae [3]. Worldwide, a total of 57.54 crore people has been infected with COVID-19 and death toll has reached up to more than 64 lakhs as on July 2022 [4]. Though SARS-CoV-2 primarily causes respiratory infection or disease which sometimes turns into severe or fatal respiratory infection and organ failure because of cytokines storm,

consequently leading to death [5]. However, the COVID-19 mostly manifested with mild to moderate flu-like symptoms such as fever, headache, cough, fatigue and a loss of sense of smell and taste [6]. Currently, there are no therapeutics available for COVID-19. Also, the emergence of post COVID-19 complications in earlier infected people raises the high demand for the prophylactic or therapeutic solutions that may prevent virus entry, replication and transmission as well as treat the lung pathologies if any. Therefore, there is a dire need for natural, safe and efficacious medicine to prevent COVID-19.

Several herbal medicines have shown potential and promising capacity against viruses by interfering with their replication cycle [7]. Also, natural compounds from plants such as flavonoids and

* Corresponding author. Department of Pharmacology, All India Institute of Medical Sciences, New Delhi, Delhi-110029, India.

E-mail addresses: bahlamuls@gmail.com (A.S. Bahl), dsarya16@gmail.com (D.S. Arya).¹ Amul S Bahl and Vipin Kumar Verma contributed equally to this work.

polyphenols are known to possess antioxidant and antiviral activity. A recent study by Hossain et al. showed several natural compounds such as amentoflavone, cepharanthine, glucogallin, aloe emodin, quercetin and berbamine showed high antiviral potential owing to their stronger interaction with both SARS-CoV-2 structural and non-structural proteins when compared to known drugs [8]. Hence, polyherbal oil having properties of inhibiting SARS-CoV-2 will be a promising therapeutic approach against COVID-19.

The detailed analysis of SAV, its composition and its role as therapeutic in patients with COVID-19 or having COVID-19 like symptom patients has been published earlier by Bahl, 2020 [9]. Briefly, Sudarshan-AV polyherbal oil was prepared using the different plants/herb/oil extract from *Origanum majorana* L., *Lavandula stoechas* L., *Mentha piperita* L., *Syzygium aromaticum* (L.) Merr. & L.M.Perry, *Ocimum basilicum* L., *Tracyspermum ammi*, *Citrus medica* L., *Mentha viridis* (L.) L., *Origanum vulgare* L., *Thymus serpyllum* L., *Cocos nucifera* L., *Helianthus annuus* L., *Sesamum indicum* L., *Allium sativum* L., *Pimpinella anisum* L. and, *Brassica campestris* L. in a definite proportion. However, the Elixir-AV oil mainly consists of essential oils from *Eucalyptus globulus* Labill., *Berberis aristata* DC, *Zingiber officinale* Roscoe, *Origanum majorana* L., *Allium sativum* L., *Melaleuca leucadendra*/*Leucadendron* (L.) L., *Thymus serpyllum* L., *Curcuma longa* L., *Lavandula angustifolia* Moench, *Hyssopus officinalis* L., *Baccharoides anthelmintica* (L.) Moench, *Vitis vinifera* L., *Melissa officinalis* L., *Brassica rapa* L., *Sesamum indicum* L. and *Helianthus annuus* L.

The gas chromatography-mass spectroscopy (GC-MS) data and identified compounds of SAV oil demonstrated that its components have antiviral, anti-inflammatory and antibacterial properties. Therefore, the previous data of polyherbal oil blends SAV along with EAV prompted us to examine its inhibition ability by *in silico* study. Several studies have reported that the SARS-CoV-2 binds to angiotensin-converting enzyme 2 (ACE2), to enter into cells [10–12]. ACE2 is an integral membrane glycoprotein expressed in various tissues mainly in lungs, heart, endothelium, and kidney [13]. The virus virion comprises structural proteins viz. Nucleocapsid (N), membrane (M), envelope (E) and spike (S) proteins. In the present study, we investigated the chemical profiling of EAV oil blend using GC-MS. Also, we investigated the molecular interaction of identified and selected 11 compounds of both SAV and EAV oil with SARS-CoV-2 components i.e., envelope, membrane and spike proteins as well as ACE 2 receptor protein of the human body, which is the host receptor of SARS-CoV-2. Further, we evaluated the efficacy of combination of two ayurvedic formulated essential oil (FEO) blends viz. SAV and EAV in hamster SARS-CoV-2 challenge model.

2. Material and methodology

2.1. EAV oil sample preparation for GC-MS analysis

The GC-MS procedure used in the present study was the same as described previously by Verma et al. [14]. Briefly, EAV oil was diluted in 1 ml of methanol (HPLC grade) followed by filtration using a 0.22 μ m syringe filter. The μ L sample was loaded by an automatic programmed syringe injector for GC-MS analysis. Further, analysis was carried out on a thermal desorption TD-20 system, GCMSQP-2010 Plus (Shimadzu, Japan). The gas chromatograph was enabled with a mass spectrometer employed with the RTx-5MS column operating in electron mode (70 eV). The carrier gas used in the instrument was helium with a flow rate of 1.2 mL/min. The initial temperature of the column was 80 °C which was, gradually increasing up to 310 °C at a steady rate at 81.7 kPa pressure. A mass spectrum was prepared with a mass scan from 40 m/z to 650 m/z at an interval of 0.5 s.

2.2. Identification of EAV oil compounds

The mass spectral database (NIST/NIH/EPA) with NIST05 (National Institute of Standards and Technology) MS program v.2.0 d and

WILEY08 libraries were used for the interpretation of GC-MS data. Based on the retention time, unknown components of the oil were identified using NIST and Wiley libraries. Also, the name, chemical formula and structure of the compound were found. The chemical and biological activity was interpreted using NCBI-PubMed, PubChem and several literatures.

2.3. Structure prediction

The protein sequences of an envelope (QJAI7754) and membrane (QJAI7755) proteins from SARS-CoV-2 were obtained from the NCBI database and subsequently, protein 3D structure prediction was carried out employing the I-Tasser web interface [15]. The predicted model structures were validated using PROCHECK [16] which provides information about Ramachandran plot statistics, backbone conformation, stereochemical quality and ERRAT program [17] which examines nonbonded atomic interactions in protein models.

2.4. Molecular docking

To gain structural insights and understand the binding mode of compounds with target proteins, molecular docking studies were performed. Protein-ligand docking was performed for all 11 compounds with target proteins from SARS CoV2- Spike (S1) (PDB ID-6M0J) [18], envelope (E) and membrane (M) proteins as well as the angiotensin-converting enzyme 2 (ACE2) receptor (PDB ID-6M0J) from humans. The 2D chemical structures of compounds were obtained from the PubChem database [19]. Before molecular docking, ligand structures were prepared using the LigPrep module from Schrodinger involving conversion from 2D to 3D form, ionization, tautomer and stereoisomer generation and minimization [20]. The structure of target proteins was prepared using Protein Preparation wizard (Schrodinger, LLC, New York, NY, 2019) which involved the addition of hydrogen atoms, assigning of bond orders and formation of disulphide bonds, removal of heteroatoms followed by energy minimization and refinement. The binding site for envelope and membrane proteins was identified using CASTp [21] web tool while interface residues of the spike-ACE2 complex were selected for grid generation for docking (Table 1). Subsequently, molecular docking was done using the Extra-Precision (XP) mode of Glide [22] where ligand molecules were docked into the binding site. A binding free energy (ΔG) score which is cumulative of several intermolecular forces was further estimated for each docked pose using the Prime MM-GBSA method [23].

2.5. Animal ethics and biosafety statement

6–8 weeks old male golden Syrian hamsters were acclimatized in biosafety level-2 (BSL-2) small animal facility (SAF) at Translational Health Science and Technology Institute (THSTI) in Faridabad, India for one week prior to challenge study (designated laboratory to conduct experiments on SARS-CoV-2, approved from ICMR-New Delhi and Department of Biotechnology, Govt. of India). During the pre-treatment

Table 1
Residues used as binding site for molecular docking.

Protein	Binding site residues
Envelope protein (CASTp predicted)	Leu 34, Thr35, Leu 51, Val 52, Phe 56, Val 58, Leu 74, Val 75
Membrane protein (CASTp predicted)	Leu 102, Arg 05, Thr106, Arg 107, Val 122, Pro 123, Leu 124, Leu 129, Leu 133, Ser 136, Ile 168, Val 170, Tyr178, Tyr179, Lys 180, Gly 182, Ala 183, Ser 184
Spike protein ACE2	Receptor binding domain (amino acids- 437–503) Ser 19, Gln 24, Thr27, Phe 28, Asp 30, Lys 31, His 34, Glu 35, Glu 37, Asp 38, Tyr41, Leu 45, Leu 79, Met 82, Tyr83, Asn 330, Lys 353, Gly 354, Asp 355, Arg 357, Arg393

regime animals were housed at SAF and then transferred to animals BSL3 (ABSL-3) institutional facility. The animals were maintained under 12 h light and dark cycle and fed a standard pellet diet and water ad libitum. All the experimental protocols involved in the handling of virus culture and animal infection were approved by RCGM (Review Committee on Genetic Manipulation), institutional biosafety, and animal ethics committee (IAEC/THSTI/118).

2.6. Virus culture and titration

SARS-related Coronavirus 2, Isolate USA-WA1/2020 virus was grown and titrated in Vero 246 E6 cell line cultured in Dulbecco's Modified Eagle Medium (DMEM) complete media 247 containing 4.5 g/L D-glucose, 100,000 U/L Penicillin-Streptomycin, 100 mg/L sodium 248 pyruvate, 25 mM HEPES, and 2% FBS. The stocks of the virus were plaque purified at THSTI, IDR facility inside ABSL3 following institutional biosafety guidelines.

2.7. SARS-CoV-2 infection in golden syrian hamster and treatment regime

A total of 23 male golden Syrian hamsters randomly allotted to different treatment groups viz. Unchallenged control (Group 1; n = 3), Infected/challenged control (Group 2; n = 5), remdesivir @15 mg/kg treatment group after infection (Group 3; n = 5), FEO treatment group after infection (Group 4; n = 5) and pretreatment FEO group before infecting the hamster with SARS-CoV-2 (Group 5; n = 5). Animals were housed in separate cages. The therapeutic group (O) received oil blends from the day of challenge while pre-treatment group (PFEO) started receiving oil blends 3 days prior to the challenge. Treatment was continued till end point for both the groups twice per day after challenge. 0.25 ml of oil A and oil B were used per dose wherein oil A was applied and rubbed from the top of the head to the end of the spine while oil B was applied and rubbed from the beginning of the neck till the tail. Both oils were topically applied and rubbed for 15–20 s. On the day of the challenge, the animals were shifted to ABSL3. All the animals, except unchallenged control, were challenged with 10^5 PFU of SARS-CoV-2 intranasal administration through catheter 50 μ l under anesthesia by using ketamine (150 mg/kg) and xylazine (10 mg/kg) intraperitoneal injection inside ABSL3 facility. Briefly, the methodology is illustrated in Fig. 1.

2.8. Gross clinical parameters of SARS-CoV-2 infection

All infected animals were euthanized on the 4th day post infection at ABSL3. Changes in body weight were observed on each day post-challenge and plotted as percent change in the body weight. Post sacrifice, lungs and spleen of the animals were excised and imaged for gross morphological changes. Right lower lobe of the lung was fixed in 10% formalin and used for histological analysis. Spleen was homogenized in 2 ml of Trizol solution. The Trizol samples were stored immediately at -80°C until further use. Blood of the animals was drawn through direct heart puncture and serum was isolated and stored at -80°C until further use.

2.9. Lung histo-pathology

The lung of the euthanized animals was fixed in 10% formalin solution and embedded in paraffin. Samples embedded paraffin blocks were then sliced transversely into 3 μm thick sections. Then, the slides were stained with hematoxylin and eosin. Each stained sample was then analyzed and captured at 40 \times magnification under light microscope (Dewinter Technologies, Italy). Assessment for the histological score was carried out through blind scoring for pneumonitis, alveolar epithelial cell injury, inflammation, and lung injury on the scale of 0–5 for each sample by an expert pathologist.

2.10. Quantitative real-time PCR

RNA was isolated from spleen samples using Trizol-choloroform method. Thereafter, RNA was quantitated by NanoDrop and 1 μg of total RNA was then reverse-transcribed to cDNA using the iScriptTM cDNA synthesis kit (Biorad; #1708891). Diluted cDNAs (1:5) was used for qPCR by using KAPA SYBR[®] FAST qPCR Master Mix (5X) Universal Kit (KK4600) on Fast 7500 Dx real-time PCR system (Applied Biosystems) and the results were analyzed with SDS2.1 software. The relative expression of each gene was expressed as fold change and was calculated by subtracting the cycling threshold (Ct) value of hypoxanthine-guanine phosphoribosyltransferase (HGPRT-endogenous control gene) from the Ct value of target gene (ΔCT). Fold change was then calculated according to the formula $\text{POWER}(2, -\Delta\text{CT}) \times 10,000$ [24]. The details of the primers are given in Supplementary Table 1.

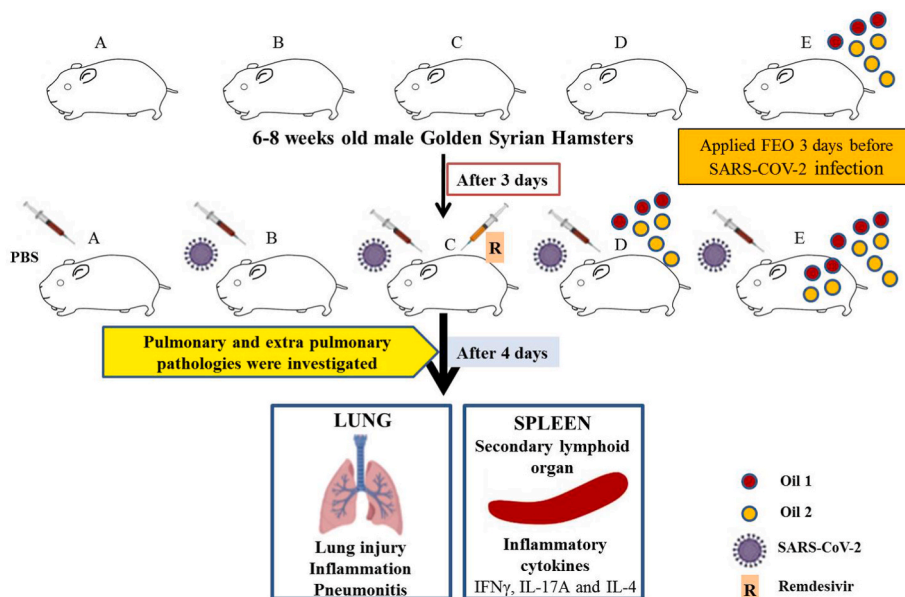


Fig. 1. An illustrative flow diagram showing the methodology.

3. Results

3.1. GC-MS analysis of EAV oil

GC-MS analysis of EAV oil, resolved in 18 major peaks (Supplementary Fig. 1) containing different compounds. The retention time and % peak area of all 18 and 15 compounds of EAV and SAV are given in Supplementary Table 2 and Supplementary Table 3 respectively. Total 12 compounds of both SAV and EAV oil with known valuable properties such as antiviral, anti-inflammatory and antibacterial as given in Supplementary Table 4 were selected. Since 1 compound (cinnamaldehyde) was common in both the oils, therefore a total of 11 compounds were investigated for molecular docking with SARS-CoV-2 components and ACE2 protein.

3.2. Structure prediction

Three-dimensional structures of SARS-CoV-2 envelope (75 aa) and membrane (222 aa) proteins were successfully predicted using a hierarchical Iterative Threading Assembly approach via the I-Tasser web server. The server provided five models with varying confidence (C) scores for each protein among which the predicted protein model with the highest C-score which also indicates its closeness to native experimental structures was chosen for further analysis in each case. Structure validation statistics revealed predicted models for both envelope protein and membrane protein were of good quality having ERRAT quality factors of 91.04 and 90.68, respectively along with 67.1 and 66.2% residues in favorable regions of the Ramachandran plot.

3.3. Molecular docking

Molecular docking of 11 compounds obtained from oils (SAV and EAV) with structural proteins as well as ACE2 was performed to determine their binding mode and thus effectiveness in the treatment of COVID-19 infection. The binding free energy (ΔG) data suggested strong binding of *trans*-beta-ocimene with envelope protein with value -25.86 kcal/mol while eugenol, *p*-cymene and thymol displayed similar binding with membrane protein with value -24.58 kcal/mol, -24.31 kcal/mol and -24.91 kcal/mol, respectively. In addition to this, cinnamaldehyde showed the most significant interaction with spike protein with value -25.87 kcal/mol (Table 2). Among the compounds cinnamaldehyde and geranial showed significant binding free energy values of -30.66 kcal/mol and -30.59 kcal/mol, respectively. Residue Arg393 in ACE2 appeared as an important binding mediator displaying hydrogen bonding with cinnamaldehyde and also geranial. The residues

Table 2
Molecular docking of compounds with target proteins.

S. No.	Ligands	Envelope protein	Membrane protein	Spike protein	ACE2
1.	Cinnamaldehyde	-5.75	-20.25	-25.87	-30.66
2.	Eucalyptol	-15.09	-21.98	NA	-12.17
3.	Eugenol	-17.87	-24.58	-22.04	-26.87
4.	Cis-beta-Ocimene	-12.40	-18.53	-14.32	-25.28
5.	Trans-Beta-Ocimene	-25.86	-23.97	-16.62	-22.76
6.	Limonene	-14.95	-18.33	-17.87	-23.60
7.	Bicyclo (4.1.0) Hept-3-ene 3,7,7 Trimethyl	-21.70	-20.27	-17.30	-15.75
8.	<i>m</i> -Cymene	-19.83	-20.85	-18.20	-24.67
9.	<i>p</i> -Cymene	-19.86	-24.31	-18.55	-22.21
10.	Thymol	-18.65	-24.91	-19.79	-28.22
11.	Geranial	-18.36	-22.44	-22.99	-30.59
12.	Known inhibitor/agonist	-	-	-30.85 (DRI-C23041)	-12.71 (metformin)

**binding energy values (in kcal/mol) of protein-ligand complexes.

significantly contributing to hydrophobic interactions in compounds-ACE2 complexes included Phe 32, Ala 36, Phe 40, Trp 69, Leu 73, Ala 99, Phe 356, Tyr385, Ala 386, Phe 390, Leu 391 and Leu 392 (Fig. 2).

3.4. FEO ameliorates infection associated gross clinical parameters

Gross clinical parameters were recorded between all the groups i.e. Control, Infected control (I), therapeutic group 3 and FEO treatment groups (group 4 and 5).

A decrease in body weight of SARS-CoV-2-infected hamsters was observed from 5 to 8% on 4 days post infection (dpi). Hamsters receiving remdesivir (I + R), formulated essential oil (I + FEO) and prophylactic formulated essential oil (I + PFEO), did not lose body weight as observed in the infected group (Fig. 3).

3.5. FEO reduces histopathological lung scores in infected hamster

Histological results indicated reduction in inflammation, alveolar injury and pneumonitis in the excised lungs of therapeutic group 4 and 5 as compared to infection control (group 2). Representative histological lung images are shown in Fig. 4. The scoring percentage for each lung lesions is shown in Fig. 5A-D. Briefly, the lung tissue of the hamster from the infected group was characterized by severe lung injury, lung inflammation, alveolar epithelial injury and pneumonitis. However, significant decrease in severity was found in the infected therapeutic group (I + FEO) and pretreated infected group (I + PFEO) ($p < 0.05$). The lung tissue of the hamster from the untreated control group did not show any lung lesions. Overall, histopathological disease score analysis also revealed that the therapeutic group (I + FEO) (group 4) and pretreated group (I + PFEO) (group 5), had 40% less average disease score as compared to the Infected group. This concluded the significant improvement in lung health due to the topical use of formulated essential oil (Fig. 6).

3.6. FEO reduces the viral load in infected hamster

We tested splenomegaly between different groups and found that treated with remdesivir group (I + R), the therapeutic group (I + FEO) and pre-treated group (I + PFEO), showed inhibition in splenomegaly as compared to the SARS-CoV2 infected hamsters (Fig. 7). The viral load at 4 dpi by qPCR showed significant reduction in viral load in treatment groups as compared to the infected group. The results showed a significantly higher viral load in the spleen of the infected group compared to that in spleen of pre-treated group (I + PFEO) and infected hamster treated with remdesivir group ($p < 0.05$) as shown in Fig. 7B. Pre-treated group with formulated essential oil significantly lowered the viral load ($P < 0.05$).

3.7. FEO inhibits the expression of pro-inflammatory cytokines

Cytokines expression data from splenocytes indicates elevated expression of IFN- γ , IL-4 and IL-17A in the infected group as compared to the control group (Fig. 8A, B and 8C). The topical application of FEO in infected hamsters resulted in the reduction in IL-4 and IL-17A cytokines expression (Fig. 8A and 8C) in therapeutic and pre-treated groups. Further, we found a significant elevated IFN- γ secretion in pre-treated group (Fig. 8B) as compared to infected groups. Together, we analyzed that FEO either applied after virus challenge or applied before virus challenge reduces the pro-inflammatory cytokines.

4. Discussion

Presently, vaccination is the only way in combating the burden of COVID-19 pandemic. However, outbreak of infection and a rampaging rise in Delta, Omicron and other new variants still remain a cause of concern [25–28]. Therefore, the demand to seek for therapeutics to

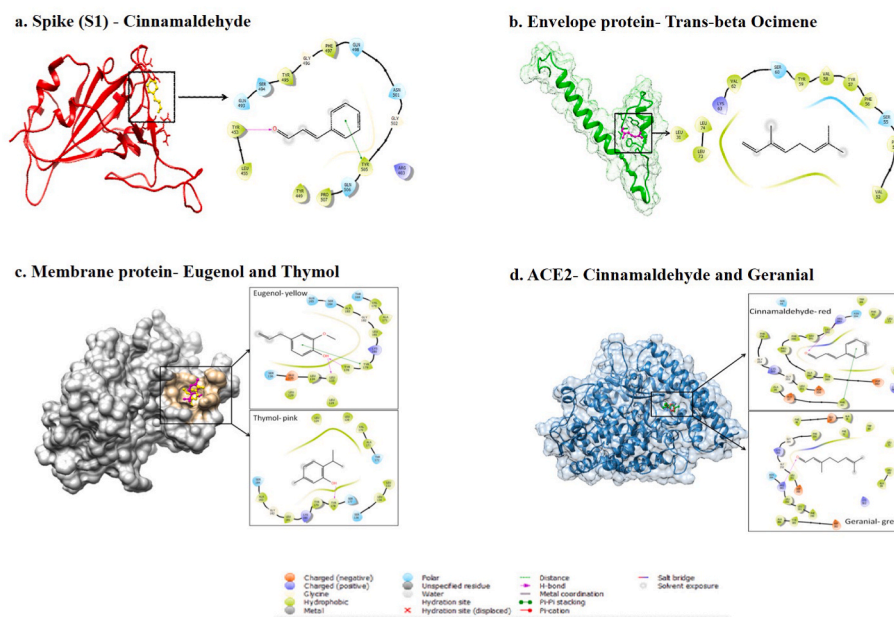


Fig. 2. Diagrammatic representation of docked complexes along with ligand interaction maps (within 0.5 nm).

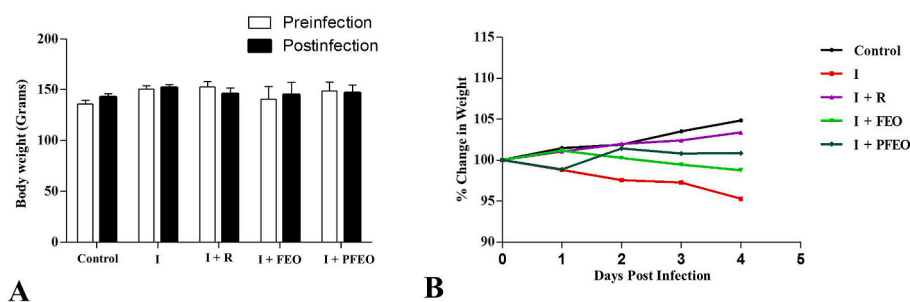


Fig. 3. (A) Body weight at the beginning and the end of the experiment; (B) Percent change in body weight w.r.t. initial weight at the time of challenge. I [Infected]; I + R [Infected + Remdesivir]; I + FEO [Infected + Formulated Essential Oil]; I + PFEO [Infected + Prophylactic Formulated Essential Oil].

prevent COVID-19 infections is of great concern along with the drug which can improve or sustain the lung pathology or overall health of the individual.

In the present study, a total 11 compounds of both SAV and EAV oil were found to have known valuable properties such as antiviral, anti-inflammatory and antibacterial etc. (Supplementary Table 4). Further *in silico* analysis revealed the binding of these 11 compounds with both ACE2 receptor and SARS-CoV-2 components. The structural proteins of SARS-CoV-2 namely envelope (E) protein, membrane (M) protein and spike (S) protein serve as important drug targets [29]. S glycoprotein binds to the host cell receptor, ACE2 via the receptor-binding domain (RBD) and has a critical role in virus entry [30–33]. The E protein is a component of the virus membrane and plays an important role during many stages of virus infection and replication while M protein is more prevalent within the virus membrane and plays a role during the budding process of coronaviruses [34,35]. Our data suggested that most of the compounds under study showed good binding with ACE2 receptor when compared to known agonist metformin [36]. A recent study by Hossain et al. showed the potential role of natural compounds such as amentoflavone and berbamine in binding with SARS-CoV-2 with the binding energy values of -10.1 and -10.0 kcal/mol respectively [8]. However, in our study the compounds cinnamaldehyde and geranial showed significant binding free energy values of -30.66 kcal/mol and -30.59 kcal/mol, respectively. Residue Arg393 in ACE2 appeared as an important binding mediator displaying hydrogen bonding with

cinnamaldehyde and geranial. Also, cinnamaldehyde showed binding free energy values of -25.87 kcal/mol with the spike protein while other study showed cepharanthine binding affinity with binding free energy values of -9.7 kcal/mol to the spike protein [8]. Since the *in silico* analysis depicts the role of polyherbal oil (SAV and EAV) in inhibiting SARS-CoV-2, we evaluated its role as prophylactic and therapeutic in the hamster model. Here, hamsters animal model was chosen to study SARS-CoV-2 infection as they developed similar SARS-CoV-2 related lung pathologies along with viral entry and infections in upper and lower respiratory tract as that of humans [37,38]. Hamsters were shown to be a better animal model for studying SARS-CoV-2 infection as ACE2 transgenic mice are not available.

The purpose of using two oil blends was to improve effectiveness to treat disease due to synergistic effects of polyherbal formulations. The Sarangdhar Samhita, an ayurvedic literature highlighted the importance of polyherbal formulations to improve its therapeutic effects to treat any disease and in reducing the toxicity [39]. The earlier study from our research group found that the blends of SAV and Whiff-MB (WMB) oils are effective in treating COVID-19 patients. A total of 44 confirmed COVID-19 patients along with 1238 patients having COVID-19 symptoms have been treated with SAV and WMB polyherbal oils [9]. In the present study, I + FEO group and I + PFEO group of hamsters did not show weight reduction in comparison to infected animals. A similar observation was also seen in hamsters treated with remdesivir. Since the clinical manifestation reported by SARS-CoV-2 infected patients was

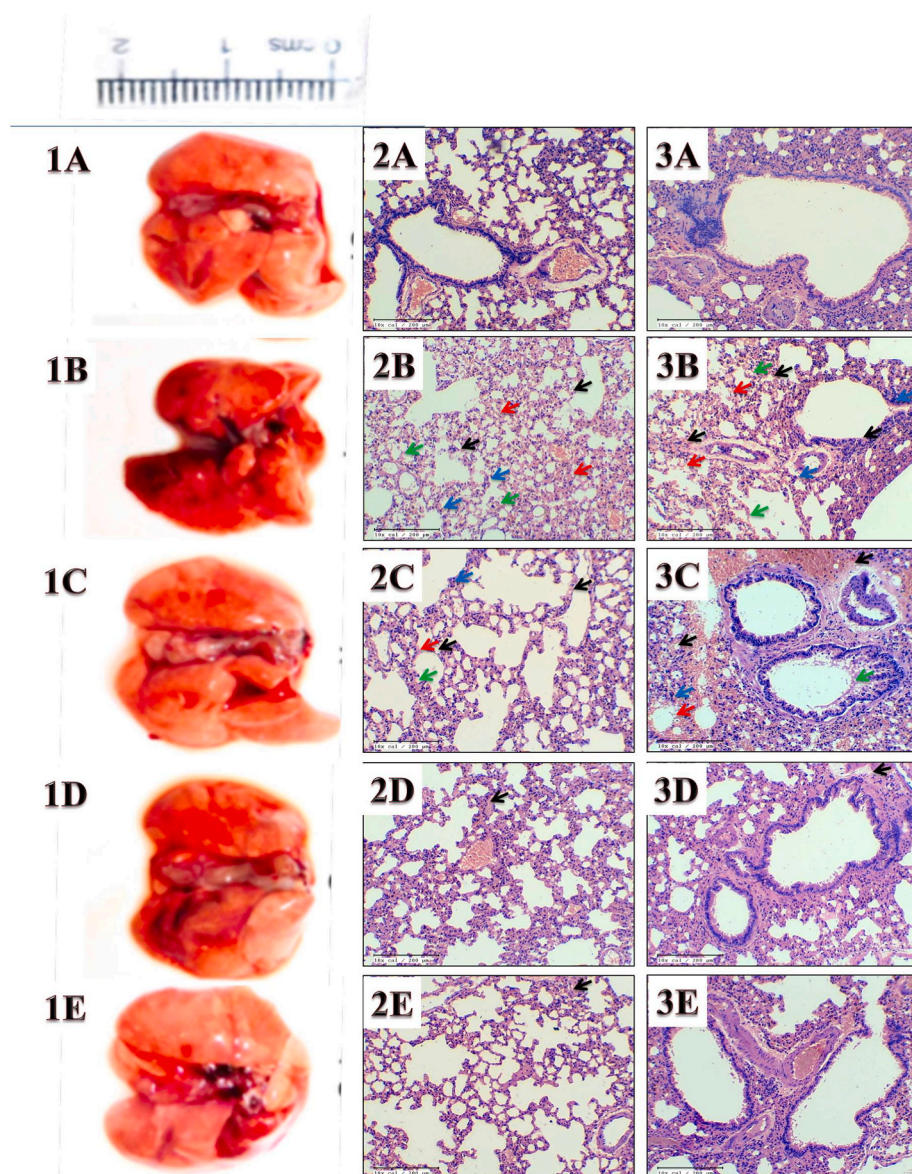


Fig. 4. Lung tissue and histopathology from each group: (A) Control; (B) I, [Infected]; (C) I + R, [Infected + Remdesivir]; (D) I + FEO [Infected + Formulated Essential Oil]; (E) I + PFEO (Infected + Prophylactic Formulated Essential Oil). 1. Dissected lung; 2. Pathological changes in lung parenchymal tissue; 3. Microscopic changes of the bronchiolar epithelium, lumen, submucosa, and peribronchiolar region. Red arrow indicate lung injury; Black arrows indicate inflammation; Green arrow indicate alveolar epithelial injury and Blue arrow indicate pneumonitis; in the histological images from respective groups.

lung injury and pneumonitis [40], we further examined the lung histopathology of infected and treated hamsters. The results from the infected group showed the severe lung injury, inflammation, alveolar epithelial cell injury and pneumonitis, however, the hamsters treated with FEO and pretreated with formulations (PFEO) showed significant decrease in lung injury. Also, reduction in the lung injury score was found in FEO treated and pretreated groups, indicating the role of polyherbal oils SAV and EAV in limiting the entry of SARS-CoV-2 along with replication of SARS-CoV-2. Also, SAV has virucidal activity which is due to the presence of benzyl alcohol which is present in high amounts (12.29%) in SAV oil. A recent study has shown the duration of viability and presence of SARS-CoV-2 on the surfaces like floors, computer mouse, sickbed handrails trash cans [41]. The lung histopathology results significantly showed the reduced inflammation, pneumonitis in infected hamsters treated with FEO which is corroborated with viral load expression indicating its role in limiting the transmission of SARS-CoV-2 infection. However, in FEO treatment group, the viral load is not significantly lower when compared infected group, the viral load study will further can be investigations in dose dependent manner or the number of times for the oil application.

Presently, most of the people who had infected with COVID-19 are

showing complications related to pulmonary systems [42]. Since, the present formulations have shown significant role in improvement in lung pathology, therefore, the FEO's could also be used to treat COVID-19 and post-COVID-19 lung complications.

The severe form of COVID-19 infection is also associated with lung inflammation due to a storm of cytokines, which is characterized by increased inflammatory markers [43]. In addition, several studies have shown the abnormal levels of cytokines and chemokines in the COVID-19 patients [44–46]. Therefore, we studied the expression of inflammatory markers. The essential cytokines in mounting immune response against a viral infection are interferons (IFN), previous study has shown that SARS-CoV-2 infection suppresses the release of IFNs *in vitro* [47]. In agreement with the previous study, decreased IFN γ expression was found in SARS-CoV-2 challenged hamsters [48], however its expression found to be significantly elevated in the hamsters treated with prophylactic formulations in comparison to both infected as well as hamsters treated with FEO, suggesting oil formulations has anti-inflammatory and immune-stimulatory effect.

In view of these findings, we report the use of SAV and EAV polyherbal formulations is efficient in combating the disastrous effects of SARS-CoV-2. The present *in vivo* study clearly indicates the preventive

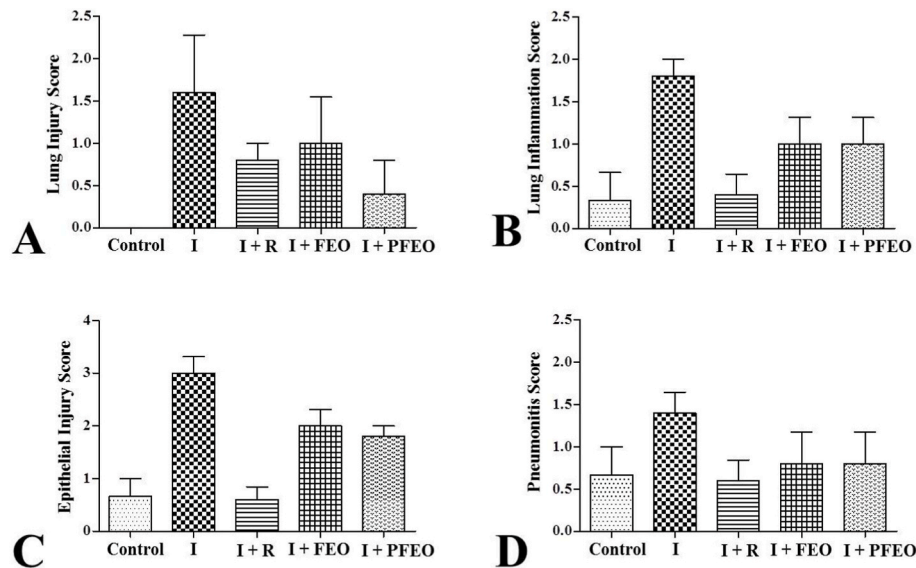


Fig. 5. Histopathological scores (grades 0 to 3, where 0 is no damage and 3 is the most damaged showing (A). Lung injury; (B). Lung inflammation; (C). Alveolar epithelial injury and (D). Pneumonitis in lung tissue from each respective groups. I [Infected]; I + R [Infected + Remdesivir]; I + FEO [Infected + Formulated Essential Oil]; I + PFEO [Infected + Prophylactic Formulated Essential Oil].

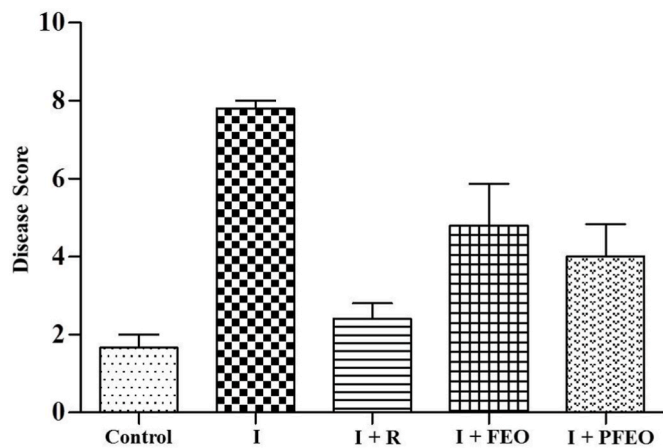


Fig. 6. Histopathological disease scores in lung tissue from respective group. I [Infected]; I + R [Infected + Remdesivir]; I + FEO [Infected + Formulated Essential Oil]; I + PFEO [Infected + Prophylactic Formulated Essential Oil].

and curative role of SAV and EAV formulations in limiting the viral load and in treatment of lung injury suggesting its role as anti-viral, anti-inflammatory and immunomodulatory.

5. Conclusion

In silico results suggest that polyherbal oil (SAV and EAV) contributes in preventing the entry of SARS-CoV-2 into the human body. Further on the basis of *in vivo* study, we summarize the findings of our study and provide the first evidence that the polyherbal oil (SAV and EAV) if applied before SARS-CoV-2 infection, limits the viral entry and replication. On the other hand, if applied post infection results in reducing SARS-CoV-2 associated pulmonary pathologies, lung injuries, pro-inflammatory cytokines through immunomodulation and prevents/ameliorates disease pathology.

Financial support

No financial support has been received from any organization.

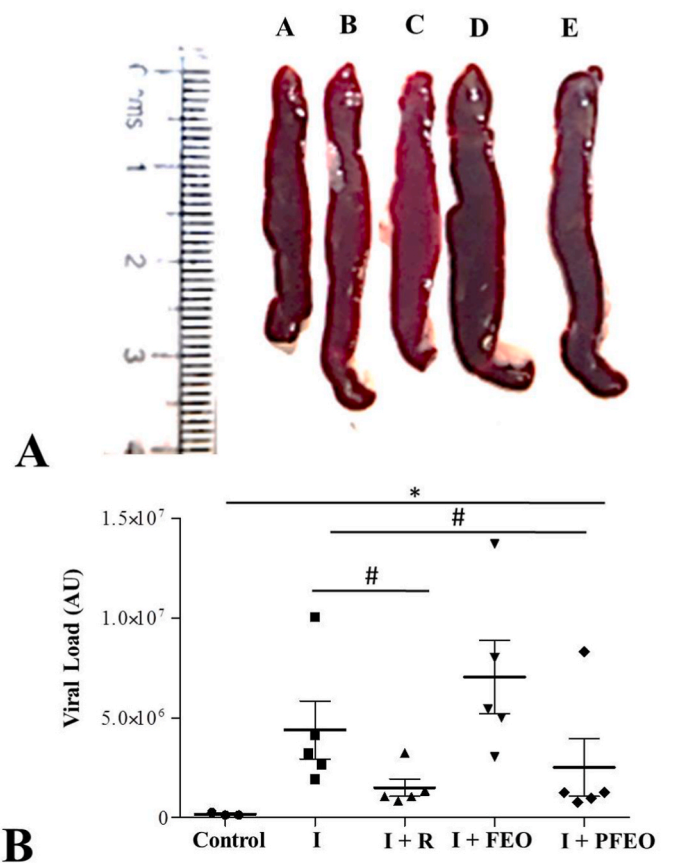


Fig. 7. A. Dissected Spleen a) Control; (b) I [Infected]; (c) I + R [Infected + Remdesivir]; (d) I + FEO [Infected + Formulated Essential Oil]; (e) I + PFEO (Infected + Prophylactic Formulated Essential Oil). B. Viral load of respective groups. Different esteries indicate statistically significant differences * vs Control; # vs Infected.

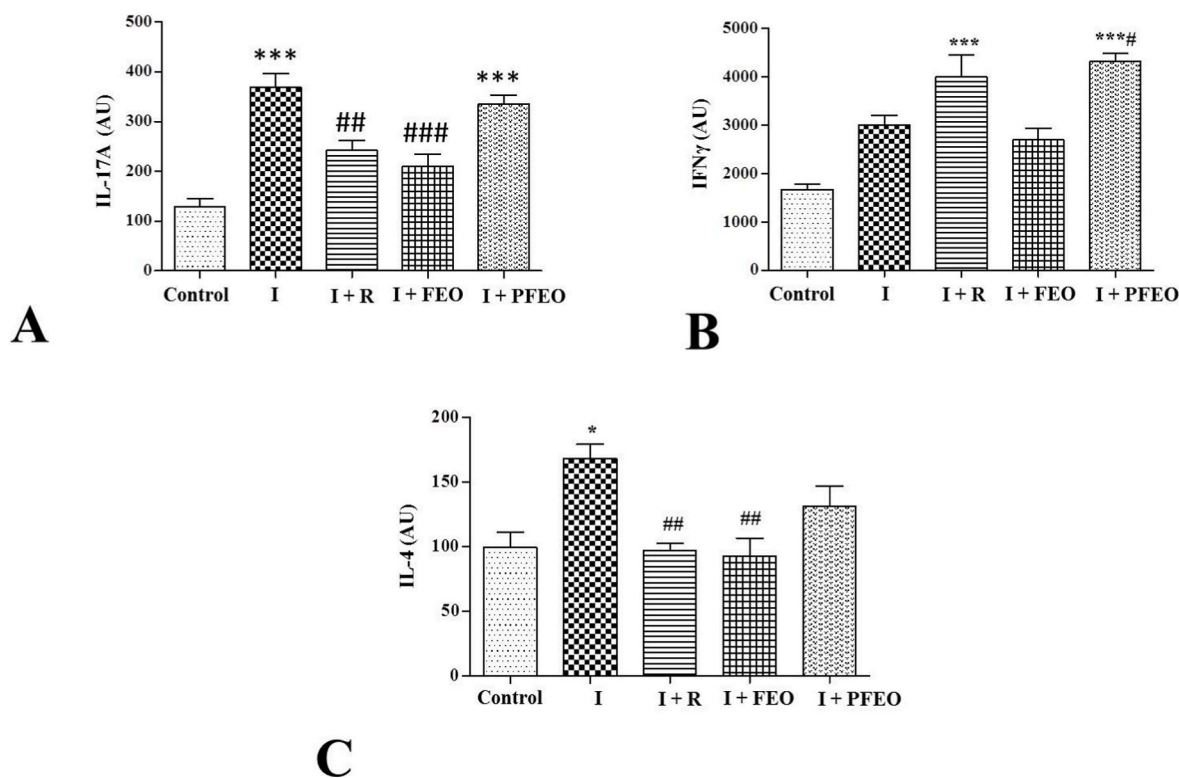


Fig. 8. Real-time qPCR expressions of IL-17A (A), IFN γ (B) and IL-4 (C) Cytokines in spleen tissue of experimental groups. Data is expressed as (mean \pm SEM). Different esteries indicate statistically significant differences * vs Control; #vs Infected. */#P < 0.05; ##P < 0.01; ***/###P < 0.001.

Declaration of competing interest

The authors declare that they have no known competing financial interests or personal relationships that could have appeared to influence the work reported in this paper.

Data availability

Data will be made available on request.

Acknowledgements

We would like to acknowledge the THSTI-Faridabad, India to conduct experimentation of animal. The work of Ms. Mansi Pandit for doing the molecular docking is also acknowledge along with Dr. Priya Bhardwaj for drafting the manuscript.

Appendix A. Supplementary data

Supplementary data to this article can be found online at <https://doi.org/10.1016/j.cbi.2022.110179>.

References

- [1] H. Lu, C.W. Stratton, Y.W. Tang, Outbreak of pneumonia of unknown etiology in Wuhan China: the mystery and the miracle, *J. Med. Virol.* 92 (4) (2020) 401–402.
- [2] Y. Huang, X. Wang, L. Li, J. Ren, Y. Zhao, Hu, et al., Clinical features of patients infected with 2019 novel coronavirus in Wuhan, China *Lancet* 395 (2020) 497–506.
- [3] Note from the editors: world Health Organization declares novel coronavirus (2019- nCoV) sixth public health emergency of international concern, *Euro Surveill.* 25 (5) (2020) 200131e.
- [4] COVID live - coronavirus statistics - worldometer. <https://www.worldometers.info/coronavirus/>. (Accessed 25 July 2022).
- [5] S. Boutin, D. Hildebrand, S. Boulant, et al., Host factors facilitating SARS-CoV-2 virus infection and replication in the lungs, *Cell. Mol. Life Sci.* 78 (16) (2021) 5953–5976.
- [6] E. Molteni, C.M. Astley, W. Ma, et al., Symptoms and syndromes associated with SARS-CoV-2 infection and severity in pregnant women from two community cohorts, *Sci. Rep.* 11 (2021) 6928.
- [7] S. Ahmad, S. Zahiruddin, B. Parveen, et al., Indian medicinal plants and formulations and their potential against COVID-19-preclinical and clinical research, *Front. Pharmacol.* 11 (2021), 578970.
- [8] R. Hossain, C. Sarkar, S.M.H. Hassan, et al., In silico screening of natural products as potential inhibitors of SARS-CoV-2 using molecular docking simulation, *Chin. J. Integr. Med.* 28 (2022) 249–256.
- [9] A.S. Bahl, Effectiveness of polyherbal topical oil treatment for patients either with 'COVID-19 like symptoms' or 'COVID-19 positive': a prospective study, *Insights Biomed* 5 (4) (2020) 13.
- [10] J. Shang, G. Ye, K. Shi, Y. Wan, C. Luo, H. Aihara, et al., Structural basis of receptor recognition by SARS-CoV-2, *Nature* 581 (7807) (2020) 221–224.
- [11] A.C. Walls, Y.J. Park, M.A. Tortorici, A. Wall, A.T. McGuire, D. Velesler, Structure, function, and antigenicity of the SARS-CoV-2 spike glycoprotein, *Cell* 181 (2) (2020) 281–292, e6.
- [12] Q. Wang, Y. Zhang, L. Wu, S. Niu, C. Song, Z. Zhang, et al., Structural and functional basis of SARS-CoV-2 entry by using human ACE2, *Cell* 181 (4) (2020 May) 894–904, e9.
- [13] M. Oz, D.E. Lorke, Multifunctional angiotensin converting enzyme 2, the SARS-CoV-2 entry receptor, and critical appraisal of its role in acute lung injury, *Biomed. Pharmacother.* 136 (2021), 111193.
- [14] V.K. Verma, N. Sehgal, O. Prakash, Characterization and screening of bioactive compounds in the extract prepared from aerial roots of *Ficus benghalensis*, *Int. J. Pharmaceut. Sci. Res.* 6 (12) (2015) 5059–5069.
- [15] J. Yang, R. Yan, A. Roy, D. Xu, J. Poisson, Y. Zhang, The I-TASSER Suite: protein structure and function prediction, *Nat. Methods* 12 (1) (2015) 8, 2015.
- [16] R.A. Laskowski, M.W. MacArthur, D.S. Moss, J.M. Thornton, PROCHECK- a program to check the stereochemical quality of protein structures, *J. Appl. Crystallogr.* 26 (1993) 283–291.
- [17] C. Colovos, T.O. Yeates, Verification of protein structures: patterns of nonbonded atomic interactions, *Protein Sci.* 2 (9) (1993) 1511–1519.
- [18] J. Lan, J. Ge, J. Yu, S. Shan, H. Zhou, S. Fan, et al., Structure of the SARS-CoV-2 Spike Receptor-Binding Domain Bound to the ACE2 Receptor, vol. 581, 2020, pp. 215–220, 7807.
- [19] S. Kim, J. Chen, T. Cheng, et al., PubChem in 2021: new data content and improved web interfaces, *Nucleic Acids Res.* 49 (D1) (2021) D1388–D1395.
- [20] G.M. Sastry, M. Adzhigirey, T. Day, R. Annabhimoju, W. Sherman, Protein and ligand preparation: parameters, protocols, and influence on virtual screening enrichments, *J. Comput. Aided Mol. Des.* 27 (3) (2013) 221–234.
- [21] W. Tian, C. Chen, X. Lei, J. Zhao, J. Liang, CASTp 3.0: computed atlas of surface topography of proteins, *Nucleic Acids Res.* 46 (W1) (2018) W363–W367.
- [22] R.A. Friesner, R.B. Murphy, M.P. Repasky, L.L. Frye, J.R. Greenwood, T.A. Halgren, et al., Extra precision glide: docking and scoring incorporating a model of

- hydrophobic enclosure for protein-ligand complexes, *J. Med. Chem.* 49 (21) (2006) 6177–6196.
- [23] G. Rastelli, A.D. Rio, G. Degliesposti, M. Sgobba, Fast and accurate predictions of binding free energies using MM-PBSA and MMGBSA, *J. Comput. Chem.* 31 (4) (2010) 797–810.
- [24] S. Malik, S. Sadhu, S. Elesela, et al., Transcription factor Foxo 1 is essential for IL-9 induction in T helper cells, *Nat. Commun.* 8 (1) (2017) 815.
- [25] K. Tyagi, A. Ghosh, D. Nair, et al., Breakthrough COVID19 infections after vaccinations in healthcare and other workers in a chronic care medical facility in New Delhi, India, *Diabetes Metabol. Syndr.* 15 (3) (2021) 1007–1008.
- [26] W.F. Garcia-Beltran, E.C. Lam, K. St Denis, et al., Multiple SARS-CoV-2 variants escape neutralization by vaccine-induced humoral immunity [published correction appears in *Cell*, *Cell* 184 (9) (2021) 2372–2383, 2021 Apr 29;184(9):2523].
- [27] D. Planas, T. Bruel, L. Grzelak, et al., Sensitivity of infectious SARS-CoV-2 B.1.1.7 and B.1.351 variants to neutralizing antibodies, *Nat. Med.* 27 (2021) 917–924.
- [28] D.A. Collier, A. De Marco, I.A.T.M. Ferreira, et al., SARS-CoV-2 B.1.1.7 sensitivity to mRNA vaccine-elicited, convalescent and monoclonal antibodies, Preprint. medRxiv. (2021) 2021, 01.19.21249840.
- [29] J. Cui, F. Li, Z.L. Shi, Origin and evolution of pathogenic coronaviruses, *Nat. Rev. Microbiol.* 17 (3) (2019) 181–192.
- [30] A. Wu, Y. Peng, B. Huang, X. Ding, X. Wang, P. Niu P, et al., Genome composition and divergence of the novel coronavirus (2019-nCoV) originating in China, *Cell Host Microbe* 27 (3) (2020) 325–328.
- [31] W. Li, M.J. Moore, N. Vasilieva, J. Sui, S.K. Wong, M.A. Berne, et al., Angiotensin-converting enzyme 2 is a functional receptor for the SARS coronavirus, *Nature* 426 (2003) 450–454.
- [32] W. Tai, L. He, X. Zhang, J. Pu, D. Voronin, S. Jiang, Y. Zhou, L. Du, Characterization of the receptor-binding domain (RBD) of 2019 novel coronavirus: implication for development of RBD protein as a viral attachment inhibitor and vaccine, *Cell. Mol. Immunol.* 17 (6) (2020) 613–620.
- [33] M. Yamamoto, S. Matsuyama, X. Li, M. Takeda, Y. Kawaguchi, J. Inoue, Z. Matsuda, Identification of nafamostat as a potent inhibitor of Middle East respiratory syndrome coronavirus S protein-mediated membrane fusion using the split-protein-based cell-cell fusion, *Assay Antimicrob. Agents and Chemotherapy* 60 (11) (2016) 6532–6539.
- [34] D. Schoeman, B.C. Fielding, Coronavirus envelope protein: current knowledge, *Virology* 16 (1) (2019) 69.
- [35] E.A. J. Alsaadi, I.M. Jones, Membrane binding proteins of coronaviruses, *Future Virology* 14 (4) (2019) 275–286.
- [36] A. Malhotra, M. Hepokoski, K.C. McCowen, J. Y-J Shyy, J. Ace2, Metformin, and COVID-19, *iScience* 23 (9) (2020), 101425.
- [37] M.E. Francis, U. Goncin, A. Kroeker, et al., SARS-CoV-2 infection in the Syrian hamster model causes inflammation as well as type I interferon dysregulation in both respiratory and non-respiratory tissues including the heart and kidney, *PLoS Pathog.* 17 (7) (2021), e1009705.
- [38] J.S. Bednash, V.E. Kagan, J.A. Englert, et al., Syrian hamsters as a model of lung injury with SARS-CoV-2 infection: pathologic, physiologic and detailed molecular profiling [published online ahead of print, 2021 Nov 2], *Transl. Res.* S1931–5244 (21) (2021), 00263-2.
- [39] A.K. Meena, P. Bansal, S. Kumar, Plants-herbal wealth as a potential source of Ayurvedic drugs, *Asian J Tradit Med* 4 (2009) 152–170.
- [40] P.H. Tsai, W.Y. Lai, Y.Y. Lin, et al., Clinical manifestation and disease progression in COVID-19 infection, *J. Chin. Med. Assoc.* 84 (1) (2021) 3–8.
- [41] Z.D. Guo, Z.Y. Wang, S.F. Zhang, et al., Aerosol and surface distribution of severe acute respiratory syndrome coronavirus 2 in hospital wards, wuhan, China, 2020, *Emerg. Infect. Dis.* 26 (7) (2020) 1583–1591.
- [42] T.K. Suvvari, L.V.S. Kutikuppala, C. Tsagkaris, A.C. Corriero, V. Kandi, Post-COVID-19 complications: multisystemic approach, *J. Med. Virol.* 93 (12) (2021) 6451–6455.
- [43] J.B. Moore, C.H. June, Cytokine release syndrome in severe COVID-19, *Science* 368 (364) (2020) 473–474.
- [44] M. Cascella, M. Rajnik, A. Aleem, et al., Features, Evaluation, and Treatment of Coronavirus (COVID-19) [Updated 2021 Sep 2]. in: *StatPearls [Internet], Treasure Island (FL): StatPearls Publishing, 2021 Jan.* <https://www.ncbi.nlm.nih.gov/books/NBK554776/>.
- [45] K. Liu, Y.Y. Fang, Y. Deng, et al., Clinical characteristics of novel coronavirus cases in tertiary hospitals in Hubei Province, *Chin. Med. J.* 133 (9) (2020) 1025–1031.
- [46] J. Wang, M. Jiang, X. Chen, L.J. Montaner, Cytokine storm and leukocyte changes in mild versus severe SARS-CoV-2 infection: review of 3939 COVID-19 patients in China and emerging pathogenesis and therapy concepts, *J. Leukoc. Biol.* 108 (1) (2020) 17–41.
- [47] Y. Liu, Y. Yang, C. Zhang, et al., Clinical and biochemical indexes from 2019-nCoV infected patients linked to viral loads and lung injury, *Sci. China Life Sci.* 63 (3) (2020) 364–374.
- [48] C.K. Yuen, J.Y. Lam, W.M. Wong, L.F. Mak, X. Wang, H. Chu, J.P. Cai, D.Y. Jin, K. K. To, J.F. Chan, K.Y. Yuen, K.H. Kok, SARS-CoV-2 nsp 13, nsp 14, nsp 15 and orf 6 function as potent interferon antagonists, *Emerg. Microb. Infect.* 9 (1) (2020 Dec) 1418–1428.